The biomass burning contribution to climate-carbon cycle feedback

Harrison, S. P. ORCID: https://orcid.org/0000-0001-5687-1903, Bartlein, P. J., Brovkin, V., Houweling, S., Kloster, S. and Prentice, I. C. (2018) The biomass burning contribution to climate-carbon cycle feedback. Earth System Dynamics, 9. pp. 663-677. ISSN 2190-4987 doi: 10.5194/esd-9-663-2018 Available at https://centaur.reading.ac.uk/75738/

Earth Syst. Dynam. Discuss., https://doi.org/10.5194/esd-2018-11
Manuscript under review for journal Earth Syst. Dynam.
Discussion started: 26 February 2018

The biomass burning contribution to climate-carbon cycle feedback

Sandy P. Harrison[1], Patrick J. Bartlein[2], Victor Brovkin[3], Sander Houweling[4], Silvia Kloster[3], I. Colin Prentice[5]

[1]Department of Geography and Environmental Science, University of Reading, Whiteknights, Reading, RG6 6AB, UK
[2]Department of Geography, University of Oregon, Eugene, Oregon 97403–1251, USA
[3]Max Planck Institute for Meteorology, Bundesstraße 53, 20146 Hamburg, Germany
[4]Department of Earth Sciences, Vrije Universiteit Amsterdam, De Boelelaan 1085, 1081 HV Amsterdam, The Netherlands
[5]AXA Chair of Biosphere and Climate Impacts, Department of Life Sciences, Imperial College London, Ascot, SL5 7PY, UK

Correspondence to: Sandy P. Harrison (s.p.harrison@reading.ac.uk)

Abstract. Temperature exerts strong controls on the incidence and severity of fire. Warming is thus expected to increase fire-related carbon emissions, and thereby atmospheric CO_2. But the magnitude of this feedback is very poorly known. We use a single-box model of the land biosphere to quantify this positive feedback from satellite-based estimates of biomass burning emissions for 2000–2014 CE, and from sedimentary charcoal records for the millennium before the industrial period. We derive an estimate of the centennial-scale feedback strength of 6.5 ± 3.4 ppm CO_2 per degree of land temperature increase, based on the satellite data. However, this estimate is poorly constrained, and is largely driven by the well-documented dependence of tropical deforestation and peat fires on climate variability patterns linked to the El Niño-Southern Oscillation. Palaeodata from pre-industrial times provide the opportunity to assess the fire-related climate-carbon cycle feedback over a longer period, with less pervasive human impacts. Past biomass burning can be quantified based on variations in either the concentration and isotopic composition of methane in ice cores (with assumptions about the isotopic signatures of different methane sources) or the abundances of charcoal preserved in sediments, which reflect landscape-scale changes in burnt biomass. These two data sources are shown here to be coherent with one another. The more numerous data from sedimentary charcoal, expressed as normalized anomalies (fractional deviations from the long-term mean), are then used – together with an estimate of mean biomass burning derived from methane isotope data – to infer a feedback strength of 5.6 ± 3.2 ppm CO_2 per degree of land temperature and (for a climate sensitivity of 2.8 K) a gain of 0.09 ± 0.05. This finding indicates that the positive feedback from increased fire provides a substantial contribution to the overall climate-carbon cycle feedback on centennial time scales.

1 Introduction

Fire is a natural, recurring event in most terrestrial ecosystems. About 4% of the global land area is burnt every year (Giglio et al., 2013), resulting in global CO_2 emissions of around 2 PgC per year (van der Werf et al., 2010), substantial contributions to the budgets of other direct or indirect greenhouse gases (including CH_4, CO, N_2O, ozone precursors), and further contributions to the atmospheric aerosol loading (black carbon, organic compounds). Climate-induced interannual variability in biomass burning, particularly variability associated with the El Niño-Southern Oscillation (ENSO), is an important component of the interannual variability of the atmospheric CO_2 growth rate (van der Werf et al., 2010). However, changes in biomass burning also occur in response to longer-term climate variability and trends (Marlon et al., 2008; Daniau et al., 2012). Changes in biomass burning therefore need to be taken into account in estimating the 'climate-carbon cycle feedback', the longer-term positive feedback by which global warming leads to a reduction in land carbon storage, a consequent reduction in the net uptake of CO_2 so that more CO_2 remains in the atmosphere – leading to an amplification of the initial warming (Arora et al., 2013; Cox et al., 2013; Wenzel et al., 2014). The dominant terms in the terrestrial carbon balance are gross primary production and total ecosystem respiration. The climate-carbon cycle feedback is generally attributed to the temperature-dependent balance of these two large annual fluxes (Keenan et al., 2016; Ballantyne et al., 2017; Jung et al., 2017); but this neglects the potential contribution of biomass burning, which we consider here.

Although there have been attempts to quantify the contribution of deforestation fires (Bowman et al., 2009) or the aerosol-related component of biomass burning (Arneth et al., 2010), the global-scale contribution of biomass burning to the climate-carbon cycle feedback has been quantified only once (Ward et al., 2012). That study reported a variety of feedbacks based on simulations using a single Earth System Model (ESM). Ward et al. (2012) found that the simulated total climate feedback due to fire was negative, but their conclusion rested mainly on a large (and highly uncertain: Boucher et al., 2013; Carslaw et al., 2013; Lee et al., 2016) indirect aerosol effect that exceeded the simulated fire feedback through the carbon cycle. In contrast, Arneth et al. (2010) estimated the aerosol feedback from biomass burning to be small and of uncertain sign.

Remotely-sensed observations of biomass burning offer a uniquely detailed global perspective on fire regimes. However, they cover only a limited period and our ability to use these records to derive an empirical estimate of the biomass-burning contribution to the carbon-cycle feedback is further compromised by the complexity of the controls on fire. Climate influences the occurrence and magnitude of fires on daily to seasonal time scales; both climate and fire affect vegetation productivity and hence the availability of fuel on yearly to decadal timescales; and human activities affect both fuel availability and fire spread. Burnt area and biomass burning have been shown to be extremely sensitive to spatial and temporal variations in temperature (Krawchuk et al.. 2009; Daniau et al., 2012; Bistinas et al., 2014), suggesting that the contribution of fire to the climate-carbon cycle feedback is likely to be positive. Yet burnt area has declined over the last decade. This decline has been attributed to the effects of fire suppression and landscape fragmentation outweighing the influence of climate-induced changes in biomass burning (Andela et al., 2017).

The use of palaeoclimate records obviates the problem of limited record length, and avoids those various human influences that have been so large as to dominate the fire record over at least the past 150 years (Marlon et al., 2008). Ice cores provide direct evidence for past changes in atmospheric composition, and the concentration and stable carbon-isotope composition of methane (CH_4) in ice cores have been used together to reconstruct changes in biomass burning during the last millennium:

see Rubino et al. (2016) for a review. CH_4 is released during the smouldering phase of fires, roughly in proportion to total CO_2 emission (Andreae and Merlet, 2001). Although this process is a relatively minor contributor to total atmospheric CH_4, it disproportionately influences the ^{13}C content of CH_4 because pyrogenic CH_4 carries the isotopic signature of photosynthesis. This is much less negative than that of the dominant (microbial) sources of CH_4 (Barker and Fritz, 1981). But measurements of the ^{13}C content of CH_4 in ice cores are currently available with limited temporal resolution, and are subject to large uncertainties in the isotopic fractionation factors for different CH_4 sources. The abundance of sedimentary charcoal provides an alternative and more direct measure of relative changes in biomass burning (Power et al., 2008; Harrison et al., 2010), and has been shown to mirror changes in biomass-burning CH_4 (Wang et al., 2010). Sedimentary charcoal data are far more numerous than ice-core isotopic records for the last millennium. If it is possible to establish a quantitative relationship between charcoal abundance and biomass-burning CH_4, it should then be worthwhile to exploit the greater number and temporal resolution of these records to quantify the fire contribution to the carbon-climate feedback. This is the approach we adopt in this paper. We use a single-box model of the land biosphere to derive an estimate of the contemporary biomass burning contribution to the climate-carbon cycle feedback using remote sensing-based estimates of biomass burning carbon emissions for the interval 2000–2014 CE. We then demonstrate that the charcoal and methane records of biomass burning during the pre-industrial Common Era (1–1700 CE) are in good agreement. Finally, we exploit a good correlation of normalized anomalies of global charcoal abundance with global land temperatures during the last millennium to derive an alternative estimate of the strength of the climate-carbon cycle feedback.

2 Data and methods

2.1 Remotely sensed burned area and carbon emissions

Burnt area and carbon emissions for 2000 to 2014 were derived from the GFED4s database (Randerson et al., 2015, http://www.geo.vu.nl/~gwerf/GFED/GFED4/), which provides monthly data on a 0.5° spatial grid. Although GFED4s also provides data for the pre-MODIS period 1997 to 1999, we do not include these early data because of large uncertainties in the burnt-area and emission estimates derived from older satellite sensors (Giglio et al., 2013). Carbon emissions in GFED4s are divided into source sectors: savannah, grassland and shrubland fires; boreal forest fires; temperate forest fires; deforestation fires; peatland fires, agricultural fires. Our estimates of total fire emissions include all of these sectors except agricultural fires. We also estimate the total emissions from natural sources, that is, also excluding deforestation and peatland fires. Global mean land temperatures for this period, for comparison with the fire data, were taken from the NOAA dataset: (ftp://ftp.ncdc.noaa.gov/pub/data/anomalies/anomalies/usingGHCNMv2/annual.land_ocean.90S.90N.df_1901-2000mean.dat).

2.2 Charcoal data

The sedimentary charcoal data were obtained from version GCDv3 of the Global Charcoal Database (Marlon et al., 2016). Charcoal data were read directly from the database file GCDv03_Marlon_et_al_2015.mdb. The data were processed using the protocol described in Power et al. (2010) and Blarquez et al. (2014) except that the transformed charcoal influx values (or their equivalents) were expressed as normalized anomalies (normans) or

$$N_t = (c_t^* - \bar{c}^*)/\bar{c}^* \tag{1}$$

where the c_t are the optimally Box-Cox transformed influx values from a particular record and $\bar{c}^*$ is the mean transformed influx for that record over the interval 1–1700 CE (the transformation and normalization base period). A 10-yr interval was used for pre-binning the 633 records used for the creation of the composite curve.

2.3 Methane concentration and stable carbon isotope data

Methane concentration data were taken from the composite Law Dome records (Etheridge et al., 2010). We used a composite data set of $\delta^{13}C$ of CH_4 from Ferretti et al. (2005), Mischler et al. (2009) and Sapart et al. (2012). We adopted the age models for each record as published. We then applied the 0.51‰ correction described by Sapart et al. (2012) to the Northern Hemisphere data.

2.4 Global palaeotemperature data

We calculated annual area-weighted averages of mean annual temperature anomalies for land grid points, using the 5º gridded data set of Mann et al. (2009), which covers the interval from 500 through 2006 CE. We used a base period of 1961–1990 CE to calculate anomalies. We did not use the global average of the PAGES 2k Consortium (2013) because this reconstruction is dominated by records from the Arctic and Antarctic, where there are few or no fires, prior to 800 CE. Although there are many last-millennium temperature reconstructions for the northern hemisphere, global data sets are few and the rest cover shorter time intervals than Mann et al. (2009).

2.5 Composite curves of charcoal, $\delta^{13}C$ of CH_4, CH_4 and palaeo-temperature data

The individual charcoal records have a median sampling interval of 16.75 years over the interval 1–100 CE (with 250 sites contributing data), and 16.90 years over the interval 1601-1700 CE (350 sites), for a typical sample density of over 1000 per century. The $\delta^{13}C$ of CH_4 and CH_4 records average 2.5 and 3.0 samples per century over the interval 1–500 CE, increasing to 10 per century over the interval 1601-1700 CE. The temperature data have annual resolution. Consequently, for the regression analyses we developed composite (across sites, in the case of charcoal) or smoothed curves (for the other variables) with a common sampling interval, and an appropriate smoothing-window for each series. We used the R package locfit (R Core Team, 2016; Loader, 2013) to fit these curves.

Earth Syst. Dynam. Discuss., https://doi.org/10.5194/esd-2018-11
Manuscript under review for journal Earth Syst. Dynam.
Discussion started: 26 February 2018

Data smoothing can induce spurious cross-correlations between series (Loader, 1999; Granger and Newbold, 1986), while using an overly high-resolution sampling interval can create temporal pseudoreplication (Hurlbert, 1984). Both could inflate the apparent significance of relationships among series. We chose the sampling interval and smoothing window by examining diagnostic checks of the regression analyses of charcoal (as the response variable) with temperature, or $\delta^{13}C$ of CH_4 and CH_4 (as predictors), attempting to minimize the autocorrelation of the residuals as a guard against pseudoreplication. This process led to the selection of a 50-year time step for evaluation of the smoothed curves. For the charcoal and temperature data, we selected a 50-year (half-width) fixed smoothing window, which suppresses inter-annual to decadal-scale variability in those series, while preserving longer-term variations. The $\delta^{13}C$ of CH_4 and CH_4 data are too sparse in the first part of the record to use a fixed-width smoothing window, and so we used the variable window-width or "span" approach with the span parameter equal to 0.1. This strategy led to some interpolation in the sparser parts of these records. We obtained bootstrap confidence intervals for the smoothed curves. For charcoal, we used the "bootstrap-by-site" approach described by Blarquez et al. (2014), which allows the impact of the variations in the spatial distribution of the charcoal records to be assessed, and the standard approach for the other series. The R code used to produce the composite/smoothed curves is included in the Supplementary Information.

2.6 Comparison of charcoal and methane records

The isotopic composition of atmospheric CH_4 depends on the magnitudes and isotopic discrimination factors of different contributors to the global CH_4 budget. Thus, although variations in biomass burning emission of CH_4 are expected to influence its isotopic composition, there is not a direct correspondence between isotopic composition and the biomass burning flux. The isotopic composition of CH_4 can also be influenced by changes in the magnitude and/or isotopic discrimination of other methane fluxes, of which the microbial source (methanogenesis in wetlands and wet soils, and in other anoxic environments including ruminant stomachs) dominates. Moreover, isotopic discrimination by methanogenesis shows large geographic variations, and cannot be assumed to be the same now (with widespread agricultural grazing, and draining of natural wetlands) as it was in pre-industrial times. We therefore chose to compare the CH_4 isotopic record with the charcoal record by treating the isotopic discrimination factors as unknown and using a regression approach, respecting the isotopic mass balance, to test whether the two types of record are systematically related to one another. After 1700 CE, the relationships between charcoal and temperature, and between charcoal and $\delta^{13}C$ [CH_4] and [CH_4] become significantly distorted. Regressions were therefore fitted using composite/smoothed curve data only up to and including 1700 CE.

The mass balance equation for the principal (non-fossil fuel) annual CH_4 fluxes to the atmosphere is:

$$F = F_m + F_g + F_b \tag{2}$$

where F is the total flux, F_m is the microbial flux, F_g is the geological flux (natural seepage from underground gas reservoirs), and F_b is the biomass burning flux. The isotopic mass balance equation is:

Earth Syst. Dynam. Discuss., https://doi.org/10.5194/esd-2018-11
Manuscript under review for journal Earth Syst. Dynam.
Discussion started: 26 February 2018

$$\delta = \delta_m(F_m/F) + \delta_g(F_g/F) + \delta_b(F_b/F) - \varepsilon \quad (3)$$

where δ is the isotopic signature ($\delta^{13}C$) of global atmospheric CH_4, δ_m, δ_g and δ_b are the isotopic signatures of the microbial, geological and biomass burning sources respectively and ε is the isotopic discrimination of CH_4 oxidation in the atmosphere and soils. Re-arrangement of equations (2) and (3) yields:

$$F_b = F(\delta - \delta_m + \varepsilon)/(\delta_b - \delta_m) - F_g(\delta_g - \delta_m)/(\delta_b - \delta_m). \quad (4)$$

The total flux F is related to the global CH_4 concentration M in steady state by $F = fM/\tau$ where f is the conversion factor between atmospheric concentration and mass and τ is the atmospheric lifetime of CH_4, which we assume to be constant. The geological flux can also be assumed constant (50 Tg CH_4 a^{-1} according to Schwietzke et al., 2016). The steady-state assumption is appropriate because we are considering variations over periods longer than the atmospheric lifetime of CH_4, approximately 9 years (Schwietzke et al., 2016). Equation 4 can then be resolved into the sum of three components: a constant intercept, a component proportional to M, and a component proportional to the product δM. Equation (4) also holds, with appropriate adjustment of units, if the F_b are expressed in normans; then all of the fluxes are relative to the mean value of F_b. We used ordinary linear regression of charcoal normans with M and δM as predictors to quantify the relationship between the charcoal data and CH_4 isotopic composition. The inclusion of CH_4 concentration in this analysis is essential, because variations in δ could be brought about irrespective of biomass burning by variations in F_m, which is generally much larger than F_b.

2.7 Calculation of feedback strengths and gain

The global relationship between biomass burning CO_2 emissions and temperature provides an estimate of the strength of the feedback. We define feedback strength as the equilibrium sensitivity of atmospheric CO_2 to global land temperature in ppm K^{-1}. This can be further converted to gain (Lashof et al., 1997). Following the convention established by Hansen et al. (1984), gain (g) is the product of the feedback strength and the climate sensitivity expressed in K ppm^{-1}. Then the temperature amplification $\Delta T/\Delta T_0$, where ΔT is the actual temperature change and ΔT_0 is the reference temperature change without the feedback, is:

$$\Delta T/\Delta T_0 = 1/(1 - g) \quad (5)$$

Note that this convention (Hansen et al., 1984) is widely applied in the literature on terrestrial biogeochemical feedbacks. However, an alternative convention exists in which the quantity defined in equation (5) is called the gain, while the quantity we call gain is called the feedback factor (see e.g. Roe, 2009).

The equilibrium sensitivity of atmospheric CO_2 to a change in the biomass burning flux was estimated using a box model, with parameters derived from either present-day or palaeo-relationships. The principle is that an increased rate of removal of

Earth Syst. Dynam. Discuss., https://doi.org/10.5194/esd-2018-11
Manuscript under review for journal Earth Syst. Dynam.
Discussion started: 26 February 2018

land carbon due to fire results in a reduced steady-state carbon storage and a correspondingly increased atmospheric CO_2 content. The increase in atmospheric CO_2 concentration is given to a good approximation by:

$$\Delta C \approx (W/\mathrm{NPP})\, \Delta F_b\, \mathrm{AF}/2.12 \qquad (6)$$

where ΔC is the increase in atmospheric CO_2 (ppm), W is total land ecosystem carbon storage (Pg C), NPP is total land net primary production (Pg C a^{-1}), ΔF_b is the increase in biomass burning carbon flux (Pg C a^{-1}), AF is the airborne fraction (the fraction of emitted CO_2 remaining in the atmosphere), and the factor 2.12 converts Pg C to ppm (http://cdiac.ornl.gov/pns/convert.html; Ciais et al., 2014). For the satellite era, we related ΔF_b (Pg C a^{-1}) statistically to temperature data. For the pre-industrial era, we related normalized anomalies (dimensionless) statistically to temperature data and multiplied by an estimate of the long-term mean F_b for the period up to 1600 CE (3.87 Pg C a^{-1}). This estimate was based on the calibration of the methane isotope record by Sapart et al. (2012), as follows: we multiplied the contemporary flux of 2.02 Pg C a^{-1} (the average of five satellite-based estimates from Shi et al., 2015) by the ratio of the global biomass-burning CH_4 flux inferred for 1–1600 CE (27.4 Tg CH_4 a^{-1}) to the same flux inferred from GFED4s (14.3 Tg CH_4 a^{-1}). Since feedback strength is related to timescale (Roe, 2009), we assumed an AF appropriate to the centennial time scale (Joos et al., 2013), and standard values for global net primary production and total carbon storage in vegetation, litter and non-permafrost soils. The derivation of equation (6), and details of calculations including the uncertainty propagation, are provided in the Appendix.

3 Results

3.1 Relationship between biomass burning flux and global average land temperature during the satellite era

The sensitivity of the MODIS-era biomass burning flux to temperature (Fig. 1) was obtained by regression of GFED4s annual fluxes against global (annual average) land temperature data, yielding a slope of 0.71 Pg C K^{-1} with a standard error of ± 0.34 Pg C K^{-1} (Fig. 2). Although approaching statistical significance, this relationship was weak ($R^2 = 0.25$, $p = 0.058$). The slope of the relationship however was shown to be insensitive to individual extreme years (see Supplementary Information).

3.2 Estimation of feedback strength during the satellite era

The fitted relationship of annual biomass burning flux to temperature provides an estimate of the feedback strength of 6.5 ± 3.4 ppm K^{-1} with respect to global land temperature. We took account of the greater variability of land versus global mean temperatures by means of a regression of land versus global mean temperature for 2000–2014 (Fig. 2a), yielding a slope of 1.364 ± 0.098 K K^{-1}. Correcting the estimated land-based feedback strength with this slope yielded a corrected feedback strength of 8.9 ± 4.7 ppm K^{-1}. Assuming a value of $S = 2.8$ K, the central value for climate sensitivity recently obtained by a novel emergent-constraint method (Cox et al., 2018), led to $\partial T/\partial C = S/(C \ln 2) = 0.0106$ K ppm^{-1} (evaluated at $C = 380$ ppm) and an estimated gain of 0.09 ± 0.05. (The uncertainty of the gain estimate does not include the uncertainty in *S*, which affects all estimates of gain but does not affect comparisons of gain made with the same value of *S*.)

However, if deforestation and peat fires (which account for 18-28% of emissions) were excluded from the calculations (Fig. 2b), no significant relationship of biomass burning emissions to temperature remained ($p = 0.476$). Interannual variability in tropical deforestion and peatland fires is well known to be correlated with the ENSO (van der Werf et al., 2010), whereas ENSO-related changes in temperature and precipitation are variable in sign across extratropical regions – resulting in compensatory impacts on total non-anthropogenic fire emissions, which show no clear general relationship to temperature during the satellite era (Prentice et al., 2011).

3.3 Relationship between methane and charcoal records of biomass burning

The fitted regression equation relating charcoal normans (dimensionless) to the concentration of CH_4 (M_t, ppb) and the product of the $\delta^{13}C$ of CH_4 (δ_t, ‰) with M_t ($\delta_t M_t$, ‰ ppb) is:

$$N_t = 0.0659 + 0.001\,18\,M_t + 0.000\,046\,79\,\delta_t M_t \quad (7)$$

($R^2 = 0.771$, $F = 54.04$ with 1 and 32 *df*, $p < 0.0001$). The standard errors of the fitted regression coefficients in equation (7) are as follows: ± 0.0147 for the intercept, ± 0.000 70 ppb^{-1} for the coefficient of M_t, and ± 0.000 012 37 ‰$^{-1}$ ppb^{-1} for the coefficient of $\delta_t M_t$ (see Supplementary Information for more details). The Ljung-Box statistic (Ljung and Box, 1978) is 16.9 with 12 *df* and $p = 0.15$, i.e. not significant, indicating that pseudoreplication and the possibility of spurious correlation are absent. This analysis confirms that the charcoal and methane data sources (Fig. 3) are in good agreement (Fig. 4b), and that it is therefore appropriate to use charcoal normans as an indicator for normalized anomalies of biomass burnt.

The ratio r of the coefficient of M_t to the coefficient of $\delta_t M_t$ could in principle provide an independent estimate of the microbial discrimination factor, as $\delta_m = \varepsilon - r$ by re-arrangement of equation (4). However, this calculation does not provide a strong constraint on δ_m. Assuming $\varepsilon = -6.3$‰ (Schwietzke et al., 2016) and with $r = 25.2 \pm 16.4$‰ from equation (7), δ_m is estimated as -31.5 ± 16.4 ‰. This value is small in magnitude compared to typical values around –60% (e.g. Sapart et al., 2012).

3.4 Relationship between charcoal records and global average land temperature

The fractional sensitivity of the millennium-scale biomass burning flux to temperature was obtained by regression of charcoal normans against global land temperature. The fitted regression equation relating charcoal normans and temperature (Fig. 4c) is:

$$N_t = -0.0205 + 0.158\,T_t \quad (8)$$

where the N_t are charcoal normans (dimensionless) and T_t are the area-weighted average temperatures (˚C; $R^2 = 0.646$, $F = 41.98$ with 1 and 23 *df*, $p < 0.0001$). The standard errors of the fitted regression coefficients in equation (8) are ± 0.005 for the intercept, and ± 0.024 K^{-1} for the coefficient of T_t. The Ljung-Box statistic is 16.2 with 12 *df*, and $p = 0.184$, i.e. non-significant.

3.5 Estimation of feedback strength during the pre-industrial era

Applying an estimated long-term mean value $F_b = 3.87 \pm 1.94$ Pg C a^{-1} yielded $\Delta F_b = 0.61 \pm 0.32$ Pg C a^{-1} K^{-1} and consequently $\Delta W = -24.8 \pm 13.8$ Pg C K^{-1}. The resulting estimate of feedback strength is 5.6 ± 3.2 ppm K^{-1} with respect to land temperature. A regression of land versus global mean temperatures based on the 500–1700 CE data in Mann et al. (2009) yielded a slope of 1.146 ± 0.0018 K K^{-1} (Fig. 2a). Correcting the estimated land-based feedback strength with this slope, and assuming $S = 2.8$ K as before, led to $\partial T/\partial C = S/(C \ln 2) = 0.0144$ K ppm^{-1} (evaluated at $C = 280$ ppm) and an estimated gain of 0.09 ± 0.05. The uncertainty in this value is dominated by the large uncertainty assigned to the mean pre-industrial biomass burning flux.

4 Discussion and Conclusions

Our analyses of data from the pre-industrial era yielded an estimate of the feedback strength of 5.6 ± 3.2 ppm K^{-1} for land temperature, and a gain of 0.09 ± 0.05. Our analyses for the satellite era yielded 6.5 ± 3.4 ppm K^{-1} for land temperature, and also a gain of 0.09 ± 0.05. The agreement between the two gain estimates is fortuitous, however. The pre-industrial estimate is founded on a strong relationship between charcoal data and reconstructed temperatures. Its uncertainty is largely due to uncertainty about the absolute magnitude of average biomass burning emissions in pre-industrial time. In contrast, the uncertainty of the satellite-era estimate is largely due to the weakness of the relationship between emissions and observed temperatures. Moreover this relationship is dominated by the well-known correlation of anthropogenic burning with the ENSO cycle. The period for which reliable satellite-based estimates of biomass burning emissions are available is too short to have allowed the effects of longer-term climate variability to emerge.

Many of the influences on fire have changed dramatically between pre-industrial and recent times. The geographic pattern of fire frequency shows an unambiguous decline with human population density, a relationship that holds across more than four orders of magnitude of population density (Bistinas et al., 2014; Knorr et al., 2014). Moreover, global biomass burning has declined precipitously since its peak in the mid-nineteenth century, as shown by both charcoal data (Marlon et al., 2008; Marlon et al., 2016) and carbon monoxide isotopes in ice and contemporary air (Wang et al., 2010). On the other hand, tropical deforestation and burning of peat substrates yield intense, localized pyrogenic sources of CO_2 that closely covary with interannual variation in the duration and intensity of the dry season (van der Werf et al., 2010). Our estimate of gain based on pre-industrial, centennial-scale climate variability is likely more relevant to long-term climate projections – while on the other hand, realistic estimation of future fire risks and feedbacks must consider the pervasive effects of human settlement and land use (Knorr et al., 2014).

Charcoal abundances have generally been interpreted as a measure of 'fire activity' or relative changes in the quantity of burned biomass (e.g. Power et al., 2008; Harrison et al., 2010; Daniau et al., 2012; Marlon et al., 2016). There have been some attempts to quantify the relationship between charcoal abundance and burnt area or total biomass consumed at a local scale (see e.g. Peters and Higuera, 2007; Duffin et al., 2016; Leys et al., 2017). These analyses, however, show a strong dependency on vegetation type and fire regime and the need to apply calibrations accounting for charcoal source area in the same way as for the interpretation of pollen abundances (Prentice, 1985: Sugita, 1994). Such calibrations have been made for Europe (Adolf et al., 2017). Our analyses establish that there is a relationship (R^2 = 0.77) between global charcoal abundance, expressed as normalized anomalies, and the methane isotopic record. Since emissions reflect the amount of biomass consumed by fire, which in turn is influenced by area burnt and fire intensity, these analyses support the idea that the sedimentary charcoal record – when synthesized at continental to global scales – can provide quantitative evidence for changes in the biomass burning carbon flux.

The total strength of the global land climate-carbon cycle feedback has been assessed by Arora et al. (2014), on the basis of multiple coupled climate-carbon cycle models, to be 13.1 ± 6.4 ppm K^{-1}. Our global estimate of the biomass burning contribution as 5.6 ± 3.2 ppm K^{-1}, based on the pre-industrial period, suggests that the contribution of fire emissions to the climate-carbon cycle feedback is substantial. Our estimate may even be conservative. Sapart et al. (2012) estimated the intertemporal coefficient of variation in the biomass burning CH_4 flux to be 7.3% for the period 1–1600 CE, compared to only 2.9% in the charcoal anomalies.

Some of the models in the assessment by Arora et al. (2014) included fire as an interactive process, but none considered deforestation or peat fires. A substantial component of the total contemporary land climate-carbon cycle feedback appears to be attributable to anthropogenic fires in the tropics, and their spatially coherent association with ENSO variability. This is in contrast with extratropical fire regimes, which show regionally asynchronous responses to climate variability (Prentice et al., 2011); and the response of net ecosystem exchange to warming, which is asymmetrical between low and high latitudes (Wenzel et al., 2014). The importance of deforestation and peatland fires in driving fire feedback in the recent decades suggests that measures to protect tropical forests and peatlands could appreciably reduce the magnitude of the climate-carbon cycle feedback.

The climate-carbon cycle feedback is an important benchmark for ESMs. Despite growing interest in the environmental and human drivers and impacts of fire (Bowman et al., 2009; Harrison et al., 2010; Bowman et al., 2011; Fischer et al., 2016), the global-scale contribution of biomass burning to the climate-carbon cycle feedback has been poorly quantified. Our analyses provide an independent estimate of this feedback, illustrating the use of the palaeo-record to estimate Earth System quantities that may be difficult or impossible to derive from contemporary observations.

Appendix: The box model, parameter estimates and their uncertainties

In steady state, carbon inputs to biomass and subsequently (via litter production) to soil organic matter, corresponding to net primary production (NPP), must be balanced by outputs: heterotrophic respiration, R_H and biomass burning, F_b. Here we designate rates of carbon transfer by heterotrophic respiration and biomass burning respectively as k_r and k_b, such that $k_b = F_b/W$; $k_b^* = F_b^*/W^*$ (where the asterisk denotes new steady-state values after a change in the burning rate); then $k_r = k_r^* = R_H/W = (\mathrm{NPP} - F_b)/W = (\mathrm{NPP} - F_b^*)/W^*$, assuming the impact of an altered fire frequency on NPP is small compared to its effect on W (Martin Calvo and Prentice 2015). Hence, $W^*/W = (\mathrm{NPP} - F_b^*)/(\mathrm{NPP} - F_b)$ and upon re-arrangement:

$$\Delta W = -W.\Delta F_b/(\mathrm{NPP} - F_b) \qquad \text{(A1)}$$

where $\Delta W = W^* - W$ and $\Delta F_b = F_b^* - F_b$, or to a close approximation (given $F_b \ll$ NPP),

$$\Delta W \approx -W.\Delta F_b/\mathrm{NPP}. \qquad \text{(A2)}$$

This calculation is insensitive to CO_2 effects on NPP, as an increase in NPP in steady state implies a proportionate increase in W.

Global terrestrial biosphere C is given by Ciais et al. (2014) as the sum of 450–650 Pg C (vegetation C) and 1500–2400 (soil C), i.e. 550 ± 100 Pg C and 1950 ± 450 Pg C respectively – yielding a combined uncertainty of ± 461 Pg C (18.4%) For global NPP, the two bottom-up estimates given by Prentice et al. (2001) are 59.9 and 62.6 Pg C a^{-1}, yielding a mean of 61.25 and a standard error ($n = 2$) of ± 1.35 Pg C a^{-1} (2.2%). We therefore assigned values of $W = 2500 \pm 461$ Pg C and NPP = 61.25 ± 1.35 Pg C a^{-1}.

For contemporary biomass burning C emissions (Shi et al., 2015; Table 3), five satellite-derived estimates together provide a global mean of 7391.7 Tg CO_2 a^{-1} (2.02 Pg C a^{-1}) with a standard deviation ($n = 5$) of ± 1291.2 Tg CO_2 a^{-1}, corresponding to a standard error of ± 0.157 Pg C a^{-1} (7.8%). We therefore assigned $F_b = 2.02 \pm 0.157$ Pg C a^{-1} for the satellite era. For the pre-industrial era, we estimated the long-term mean biomass burning C flux as the product of the contemporary flux of 2.02 Pg C a^{-1} (Shi et al., 2015) with the ratio of the global biomass-burning CH_4 flux inferred from methane isotope data for the period 1–1600 CE (27.4 Tg CH_4 a^{-1}) to the same flux inferred from GFED4s (14.3 Tg CH_4 a^{-1}) by Sapart et al. (2012), yielding $F_b = 3.87$ Pg C a^{-1}. However, while Sapart et al. (2012) assigned an uncertainty of only ± 2.8 Tg CH_4 a^{-1} (10%) to their estimate of global biomass-burning CH_4 flux, we inflated the uncertainty of our estimate of F_b to ± 1.94 Pg C a^{-1} (50%) in order to include additional potential sources of error, which include variability of the isotopic fractionation factors and of the emission factor for CH_4 with respect to CO_2.

For the centennial-scale airborne fraction (AF in equation 6) we adopted the estimate of 0.476 ± 0.057 (12.0%) obtained by Joos et al. (2013). This estimate was derived from multiple models performing identical pulse-response experiments. The mean value here is the multi-model mean (converted from units of years to fractions by dividing by the time scale), and the uncertainties are one standard deviation of the variation among models. The mean value is close to the empirical estimate of 0.44 given by Ciais et al. (2014).

Conversion of the feedback strength ($\partial C/\partial T$) into a gain requires a further assumption about the climate sensitivity (S), defined as the equilibrium change in global mean temperature for a doubling of atmospheric CO_2. We have used $S = 2.8$ K, the central estimate provided by Cox et al. (2018).

Data Availability. All the data used in the analyses are public, and available from the sites given in the text or references. Our analyses are fully documented in Supplementary Information.

Author Contributions. SPH, ICP, PJB and SK designed and performed the analyses. SPH and ICP wrote the first draft of the manuscript and all authors contributed to the final version.

Competing Financial Interests. There are no competing financial interests.

Acknowledgements. This work was inspired by discussions at workshops of the Global Palaeofire Working Group in 2012 and 2013, and partially funded by the University of Reading. SPH acknowledges the support from the ERC-funded project GC2.0 (Global Change 2.0: Unlocking the past for a clearer future, grant number 694481). This research is a contribution to the AXA Chair Programme in Biosphere and Climate Impacts and the Imperial College initiative on Grand Challenges in Ecosystems and the Environment (ICP). PJB acknowledges funding from the U.S. National Science Foundation Geography and Spatial Science Program (1435744).

References

Adolf, C., Wunderle, S., Colombaroli, D., Weber, H., Gobet, E., Heiri, O., van Leeuwen, J. F. N., Bigler, C., Connor, S. E., Gałka, M., La Mantia, T., Makhortykh, S., Svitavska-Svobodova, H., Vannière, B., Tinner, W.: The sedimentary and remote-sensing reflection of biomass burning in Europe, Global Ecol. Biogeogr., 2017, 1–14, DOI: 10.1111/geb.12682, 2017.

Andela, N., Morton, D. C., Giglio, L., Chen, Y., van der Werf, G. R., Kasibhatla, P. S., DeFries, R. S., Collatz, G. J., Hantson, S., Kloster, S., Bachelet, D., Forrest, M., Lasslop, G., Li, F., Mangeon, S., Melton, J. R., Yue, C., and Randerson, J. T.: A human-driven decline in global burned area, Science, 356: 1356–1362, DOI: 10.1126/science.aal4108, 2017.

Andreae, M. O., and Merlet, P.: Emission of trace gases and aerosols from biomass burning, Glob. Biogeochem. Cycl., 15, 955-966, DOI: 10.1029/2000GB001382, 2001.

Arneth, A. Harrison, S. P., Zaehle, S., Tsigaridis, K., Menon, S., Bartlein, P. J., Feichter, H., Korhola, A., Kulmala, M., O'Donnell, D., Schurgers, S., Sorvari, S., and Vesala, T.: Terrestrial biogeochemical feedbacks in the climate system, Nature Geosci., 3, 525-532, DOI: 10.1038/ngeo905, 2010.

Arora, V. K, Boer, G. J., Friedlingstein, P., Eby, M., Jones, C. D., Christian, J. R., Bonan, G., Bopp, L., Brovkin, V., Cadule, P., Hajima, T., Ilyina, T., Lindsay, K., Tjiputra, J. F., and Wu, T.: Carbon–concentration and carbon–climate feedbacks in CMIP5 Earth System Models, J. Clim., 26, 5289- 5314, DOI: 10.1175/JCLI-D-12-00494.1, 2013.

Ballantyne, A., Smith, W., Anderegg, W., Kauppi, P., Sarmiento, J., Tans, P., Shevliakova, E., Pan, Y., Poulter, B., Anav, A., Friedlingstein, P., Houghton, R., and Running, S.: Accelerating net terrestrial carbon uptake during the warming hiatus due to reduced respiration, Nature Clim. Change, 7, 148-152, DOI: 10.1038/nclimate3204, 2017.

Barker, J.F., and Fritz, P.: Carbon isotope fractionation during microbial methane oxidation, Nature, 293, 289-291, DOI: 10.1038/293289a0, 1981.

Bistinas, I., Harrison, S .P., Prentice, I. C., and Pereira, J. M. C.: Causal relationships vs. emergent patterns in the global controls of fire frequency, Biogeosci., 11, 5087-5101, doi.org/10.5194/bg-11-5087-2014, 2014.

Blarquez, O., Vanniere, B. , Marlon, J. R., Daniau, A-L., Power, M. J., Brewer, S., and Bartlein, P. J.: paleofire: An R package to analyse sedimentary charcoal records from the Global Charcoal Database to reconstruct past biomass burning, Comp. Geosci., 72, 255-261, 2014.

Boucher, O., Randall, D., Artaxo, P., Bretherton, C., Feingold, G., Forster, P., Kerminen, V.-M., Kondo, Y., Liao, H., Lohmann, U., Rasch, P., Satheesh, S. K., Sherwood, S., Stevens B., and Zhang, X.Y.: Climate and aerosols. In: Climate Change 2013: The Physical Science Basis. Contribution of Working Group I to the Fifth Assessment Report of the Intergovernmental Panel on Climate Change [Stocker, T. F., D. Qin, G.-K. Plattner, M. Tignor, S. K. Allen, J. Boschung, A. Nauels, Y. Xia, V. Bex and P. M. Midgley (eds.)]. Cambridge University Press, Cambridge, UK and New York, NY, USA (2013).

Bowman, D. M. J. S., Balch, J. K., Artaxo, P., Bond, W. J., Cochrane, M. A., D'Antonia, C. M., DeFries, R. S., Doyle, J. C., Harrison, S. P., Johnston, F. H., Keeley, J. E., Krawchuk, M. A., Kull, C. A., Marston, J. B., Moritz, M. A., Prentice, I. C., Roos, C. I., Scott, A. C., Swetnam, T. W., van der Werf, G. R., and Pyne, S. J.,: Fire in the earth system, Science, 324, 481-484, DOI: 10.1126/science.1163886, 2009.

Bowman D. M. J. S., Balch, J., Artaxo, P., Bond, W. J., Cochrane, M. A., D'Antonio, C. M, DeFries, R., Johnston, F. H., Keeley, J. E., Krawchuk, M. A. Kull, C. A., Mack, M., Moritz, M. A., Pyne, S., Roos, C. I., Scott, A. C., Sodhi, N. S., Swetnam, T. W., and Whittaker, R.:The human dimension of fire regimes on Earth, J. Biogeog., 38, 2223-2236, DOI:10.1111/j.1365-2699.2011.02595.x, 2011.

Earth Syst. Dynam. Discuss., https://doi.org/10.5194/esd-2018-11
Manuscript under review for journal Earth Syst. Dynam.
Discussion started: 26 February 2018

Carslaw, K. S., Lee, L. A., Reddington, C. L., Pringle, K. J., Rap, A., Forster, P. M., Mann, G. W., Spracklen, D. V., Woodhouse, M. T., Regayre, L. A., and Pierce, J. R.: Large contribution of natural aerosols to uncertainty in indirect forcing, Nature, 503, 67-74, doi:10.1038/nature12674, 2013.

Ciais, P., Sabine, C., Bala, G., Bopp, L., Brovkin, V., Canadell, J., Chhabra, A., DeFries, R., Galloway, J., Heimann, M., Jones, C., Le Quéré, C., Myneni, R. B., Piao, S., and Thornton, P.: Carbon and other biogeochemical cycles. In: *Climate Change 2013: The Physical Science Basis. Contribution of Working Group I to the Fifth Assessment Report of the Intergovernmental Panel on Climate Change* [Stocker, T.F., D. Qin, G.-K. Plattner, M. Tignor, S.K. Allen, J. Boschung, A. Nauels, Y. Xia, V. Bex and P.M. Midgley (eds.)]. Cambridge University Press, Cambridge, UK and New York, USA (2013).

Cox, P. M., Huntingford, C., and Williamson, M. S.: Emergent constraint on equilibrium climate sensitivity from global temperature variability, Nature, 553, 319-322, DOI: 10.1038/nature25450, 2018.

Cox, P. M., Pearson, D., Booth, B. B., Friedlingstein, P., Huntingford, C., Jones, C. D., and Luke, C. M.: Sensitivity of tropical carbon to climate change constrained by carbon dioxide variability, Nature, 494, 341–344, DOI:10.1038/nature11882, 2013.

Daniau, A.-L., Bartlein, P. J., Harrison, S. P., Prentice, I. C., Brewer, S., Friedlingstein, P., Harrison-Prentice, T. I., Inoue, J., Marlon, J. R., Mooney, S., Power, M. J., Stevenson, J., Tinner, W., Andrič, M., Atanassova, J., Behling, H., Black, M., Blarquez, O., Brown, K. J., Carcaillet, C., Colhoun, E., Colombaroli, D., Davis, B. A. S., D'Costa, D., Dodson, J., Dupont, L., Eshetu, Z., Gavin, D. G., Genries, A., Gebru, T., Haberle, S., Hallett, D. J., Horn, S., Hope, G., Katamura, F., Kennedy, L., Kershaw, P., Krivonogov, S., Long, C., Magri, D., Marinova, E., McKenzie, G. M., Moreno, P. I., Moss, P., Neumann, F. H., Norström, E., Paitre, C., Rius, D., Roberts, N., Robinson, G., Sasaki, N., Scott, L., Takahara, H., Terwilliger, V., Thevenon, F., Turner, R. B., Valsecchi, V. G., Vannière, B., Walsh, M., Williams, N., and Zhang, Y.: Predictability of biomass burning in response to climate changes, Glob. Biogeochem. Cyc., 26, DOI:10.1029/2011GB004249, 2012.

Duffin, K. I., Gillson, L., and Willis, K. J.: Testing the sensitivity of charcoal as an indicator of fire events in savanna environments: quantitative predictions of fire proximity, area and intensity. The Holocene, 18, 279–291, DOI: 0.1177/0959683607086766, 2008.

Etheridge, D.M. *et al.*: Law Dome Ice Core 2000-Year CO_2, CH_4, and N_2O Data. *IGBP PAGES/World Data Center for Paleoclimatology, Data Contribution Series* # 2010-070. NOAA/NCDC Paleoclimatology Program, Boulder CO, USA (2010). (Data available from: ftp://ftp.ncdc.noaa.gov/pub/data/paleo/icecore/antarctica/law/law2006.xls)

Ferretti, D. F., Miller, J. B., White, J. W. C., Etheridge, D. M., Lassey, K. R., Lowe, D. C., MacFarling Meure, C. M., Dreier, M. F., Trudinger, C. M., van Ommen, T. D., and Langenfelds, R. L.: Unexpected changes to the global methane budget over the past 2000 years. Science 309, 1714-1717, DOI: 10.1126/science.1115193, 2005. (Data available from: doi: 10.1126/science.1115193)

Fischer, A. P., Spies, T. A., Steelman, T. A., Moseley, C., Johnson, B. R., Bailey, J. D., Ager, A. A., Bourgeron, P., Charnley, S., Collins, B. M., Kline, J. D., Leahy, J. E., Littell, J. S., Millington, J. D. A., Nielsen-Pincus, M., Olsen, C. S., Paveglio, T. B., Roos, C. I., Steen-Adams, M. M., Stevens, F. R., Vukomanovic, J., White, E. M., and Bowman, D. M.: Wildfire risk as a socioecological pathology, Frontiers Ecol. Environ., 14, 276-284. 10.1002/fee.1283, 2016.

Giglio, L., Randerson, J. T. and van der Werf, G. R.: Analysis of daily, monthly, and annual burned area using the fourth-generation global fire emissions database (GFED4). J. Geophys. Res: Biogeosci., 118, 317-328, DOI:10.1002/jgrg.20042, 2013.

Granger, C. W. J., and Newbold, P.: Forecasting Economic Time Series. Academic Press, 2nd edition, 1986.

Hansen, J., Lacis, A., Rind, D., Russell, G., Stone, P., Fung, I., Ruedy, R., and Lerner, J.: Climate sensitivity: Analysis of feedback mechanisms, In: Climate Processes and Climate Sensitivity [J. E. Hansen, and T. Takahashi, Eds.]. AGU Geophysical Monograph 29, Maurice Ewing Vol. 5. American Geophysical Union, 130-163, 1984.

Harrison, S.P., Marlon, J., and Bartlein, P.J.: Fire in the Earth System, In: Dodson, J. (Ed.), Changing Climates, Earth Systems and Society, Springer-Verlag, 21-48, 10.1007/978-90-481-8716-4_3, 2010.

Hurlbert, S.H.: Pseudoreplication and the design of ecological field experiments, Ecological Monographs**,** 54, 187-211, DOI: 10.2307/1942661, 1984.

Joos, F., Roth, R., Fuglestvedt, J. S., Peters, G. P., Enting, I. G., von Bloh, W., Brovkin, V., Burke, E. J., Eby, M., Edwards, N. R., Friedrich, T., Frölicher, T. L., Halloran, P. R., Holden, P. B., Jones, C., Kleinen, T., Mackenzie, F. T., Matsumoto, K., Meinshausen, M., Plattner, G.-K., Reisinger, A., Segschneider, J., Shaffer, G., Steinacher, M., Strassmann, K., Tanaka, K., Timmermann, A., and Weaver, A. J.:Carbon dioxide and climate impulse response functions for the computation of greenhouse gas metrics: a multi-model analysis, Atmos. Chem. Phys., 13, 2793-2825, https://doi.org/10.5194/acp-13-2793-2013, 2013.

Jung, M., Reichstein, M., Schwalm, C. R., Huntingford, C., Sitch, S. Ahlström, A., Arneth, A., Cams-Valls, G., Ciais, P., Friedlingstein, P., Gans, F., Ichii, K., Jain, A. K., Kato, E., Papale, D., Poulter, B., Raduly, B., Rödenbeck, C., Tramontana, G., Viovy, N., Wang, Y-P., Weber, U., Zaehle, S., and Zeng, N.: Compensatory water effects link yearly global land CO_2 sink changes to temperature, Nature, 541, 516-520, DOI: 10.1038/nature20780, 2017.

Keenan, T. F., Prentice, I. C., Canadell, J. G., Williams, C. A., Wang, H., Raupach, M., and Collatz, G. J.:. Recent pause in the growth rate of atmospheric CO_2 due to enhanced terrestrial uptake, Nature Comms., DOI: 10.1038/ncomms13428, 2016.

Knorr, W., Kaminski, T., Arneth, A., and Weber, U.: Impact of human population density on fire frequency at the global scale, Biogeosci., 11, 1085-1102, https://doi.org/10.5194/bg-11-1085-2014, 2014.

Krawchuk, M., Moritz, M., Parisien, M.-A., Van Dorn, J., and Hayhoe, K.: Global pyrogeography: The current and future distribution of wildfire, PLoS ONE **4**, e5102, https://doi.org/10.1371/journal.pone.0005102, 2009.

Lashof, D. A., DeAngelo, B. J., Saleska, S .R., and Harte, J.: Terrestrial ecosystem feedbacks to global climate change. Annu. Rev. Energy Environ.**,** 22, 75–118, DOI: 10.1146/annurev.energy.22.1.75, 1997.

Lee, L. A., Reddington, C. L., and Carslaw, K. S.: On the relationship between aerosol model uncertainty and radiative forcing uncertainty, PNAS, 113, 5820-5827, DOI 10.1073/pnas.1507050113, 2016.

Leys, B.A, Commerford, J. L., and McLauchlan, K. K.: Reconstructing grassland fire history using sedimentary charcoal: Considering count, size and shape, PLOSONE, 12, e0176445, https://doi.org/10.1371/journal.pone.0176445, 2017.

Loader, C.: Local Regression and Likelihood, Springer, 1999.

Loader, C.: locfit: Local Regression, Likelihood and Density Estimation. R package version 1.5-9.1. https://CRAN.R-project.org/package=locfit, 2013.

Ljung, G., and Box, G. E. P.: On a measure of lack of fit in time series models, Biometrics, 65, 297-303, http://dx.doi.org/10.1093/biomet/65.2.297, 1978.

Martin Calvo, M., and Prentice, I. C.: Effects of fire and CO_2 on biogeography and primary production in glacial and modern climates, New Phytol., 208, 987-994, DOI: 0.1111/nph.13485, 2015.

Mann, M.E., Zhang, Z., Rutherford, S., Bradley, R. S., Hughes, M/ K., Shindell, D., Ammann, C., Faluvegi, G., and Ni, F.: Global signatures and dynamical origins of the Little Ice Age and Medieval Climate Anomaly, Science, 326, 1256-1260, DOI: 10.1126/science.1177303, 2009. (Data available from http://science.sciencemag.org/content/suppl/2009/11/25/326.5957.1256.DC1)

Marlon, J., Bartlein, P. J., Carcaillet, C., Gavin, D. G., Harrison, S. P., Higuera, P. E., Joos, F., Power, M., Prentice, I. C.: Climate and human influences on global biomass burning over the past two millennia, Nature Geosci., 1, 697-702, DOI: 10.1038/ngeo313, 2008.

Marlon, J. R., Kelly, R., Daniau, A.-L., Vannière, B., Power, M. J., Bartlein, P. J., Higuera, P., Blarquez, O., Brewer, S., Brücher, T., Feurdean, A., Gil Romera, G., Iglesias, V., Maezumi, Y., Magi, B., Courtney Mustaphi, C. J., and Zhihai, T.: Reconstructions of biomass burning from sediment-charcoal records to improve data–model comparisons, Biogeosci., 13, 3225-3244, DOI:10.5194/bg-13-3225-2016, 2016. (Data available from: http://paleofire.org)

Mischler, J. A., Sowers, T. A., Alley, R. B., Battle, M., McConnell, J. R., Mitchell, L., Popp, T., Sofen, E., and Spencer, M. K.: Carbon and hydrogen isotopic composition of methane over the last 1000 years, Glob. Biogeochem. Cycl., 23, GB4024, DOIi: 10.1029/2009GB003460 (2009). (Data available from: ftp://sidads.colorado.edu/pub/DATASETS/AGDC/sowers_nsidc_0435/WAIS_d13C_dD%20_CH4.xls)

PAGES 2k Consortium: Continental-scale temperature variability during the past two millennia, Nature Geosci., 6, 339-346, DOI: 10.1038.ngeo1797, 2013.

Peters, M. E., and Higuera, P. E.: Quantifying the source area of macroscopic charcoal with a particle dispersal model, Quat. Res., 67, 304–10, DOI: 10.1.1.510.4324, 2007.

Power, M.J., Ortiz, N., Marlon, J., Bartlein, P. J., Harrison, S. P., Mayle, F., Ballouche, A., Bradshaw, R., Carcaillet, C., Cordova, C., Mooney, S., Moreno, P., Prentice, I. C., Thonicke, K., Tinner, W., Whitlock, C., Zhang, Y., Zhao, Y., Anderson, R. S., Beer, R., Behling, H., Briles, C., Brown, K, Brunelle A., Bush, M., Clark, J., Colombaroli, D., Chu, C. Q., Daniels, M., Dodson, J., Edwards, M. E., Fisinger, W., Gavin, D. G., Gobet, E., Hallett, D. J., Higuera, P., Horn, S., Inoue, J., Kaltenrieder, P., Kennedy, L., Kong, Z. C., Long, C., Lynch, J., Lynch, B., McGlone, M., Meeks, S., Meyer, G., Minckley, T., Mohr, J., Noti, R., Pierce, J., Richard, P., Shuman, B. J., Takahara, H., Toney, J., Turney, C., Umbanhower,

Earth Syst. Dynam. Discuss., https://doi.org/10.5194/esd-2018-11
Manuscript under review for journal Earth Syst. Dynam.
Discussion started: 26 February 2018

Earth System Dynamics
Open Access
Discussions

C., Vandergoes, M., Vanniere, B., Vescovi, E., Walsh, M., Wang, X., Williams, N., Wilmshurst, J., and Zhang , J.H.: Changes in fire activity since the LGM: an assessment based on a global synthesis and analysis of charcoal data. Climate Dynamics, 30, 887-907, DOI: 10.1007/s00382.00.0334x, 2008.

Power, M. J., Marlon, J. R., Bartlein, P. J., and Harrison, S. P.: Fire history and the Global Charcoal Database: A new tool for hypothesis testing and data exploration, Palaeoclim., Palaeogeog. Palaeoecol., 291, 52-59, DOI: https://doi.org/10.1016/j.palaeo.2009.09.014, 2010.

Prentice, I. C.: Pollen representation, source area, and basin size: toward a unified theory of pollen analysis, Quat. Res., 23: 76-86, DOI: 10.1016/0033-5894(85)90073-0, 1985.

Prentice, I. C., Farquhar, G. D., Fasham, M. J. R., Goulden, M. L., Heimann, M., Jaramillo, V. J., Kheshgi, H. S., Le Quéré, C., Scholes, R. J., and Wallace, D. W. R.: The carbon cycle and atmospheric carbon dioxide. In: Climate Change 2001: The Scientific Basis (J.T. Houghton, Y. Ding, D.J. Griggs, M. Noguer, P.J. van der Linden, X. Dai, K. Maskell and C.A. Johnson, eds). Cambridge University Press, Cambridge, 183-237, 2001.

Prentice, I. C., Kelley, D. I., Foster, P. N. Friedlingstein, P., Harrison, S. P., and Bartlein, P. J.: Modeling fire and the terrestrial carbon balance, Glob. Biogeochem. Cycl., 25, GB3005, doi:10.1029/2010GB003906, 2011.

R Core Team. R: A language and environment for statistical computing. R Foundation for Statistical Computing, Vienna, Austria. URL https://www.r-project.org/, 2016.

Randerson, J. T., van der Werf, G. R., Giglio, L., Collatz, G. J., and Kasibhatla, P. S.: Global Fire Emissions Database, Version 4, (GFEDv4). ORNL DAAC, Oak Ridge, Tennessee, USA. http://dx.doi.org/10.3334/ORNLDAAC/1293, 2015.

Roe, G.: Feedbacks, timescales, and seeing red. Annu. Rev. Earth Planet. Sci, 37, 93–115, DOI: 10.1146/annurev.earth.061008.134734, 2009.

Rubino, M., D'Onofrio, A., Seki, O., and Bendle, J. A.: Ice-core records of biomass burning, Anthrop. Rev., 3: 140–162, https://doi.org/10.1177/2053019615605117, 2016.

Sapart, C. J., Monteil, G., Prokopiou, M., van der Wal, R. S. W., Kaplan, J. O., Sperlich, P., Krumhardt, K. M., van der Veen, C., Houweling, S., Krol, M. C., Bluneir, T., Sowers, T., Martinerie, P., Witrant, E., Dahl-Jensen, D., and Röckmann, T.: Natural and anthropogenic variations in methane sources during the past two millennia, Nature, 490, 85-88, DOI: 10.1038/nature11461, 2012.

Schwietzke, S. Sherwood, O. A., Bruhwiler, L. M. P., Miller, J. B., Etiope, G., Dlugokencky, E. J., Michel, S. E., Arling, V. A., Vaughn, B. H., White, J. W. C., and Tans, P. P.: Upward revision of global fossil fuel methane emissions based on isotope database. *Nature* **538**, 88-91, doi: 10.1038/nature19797 (2016).

Shi, Y., Matsunaga, T., Saito, M., Yamaguchi, Y., and Chen, X.: Comparison of global inventories of CO_2 emissions from biomass burning during 2002–2011 derived from multiple satellite products, Environ. Poll., 206, 479-487, https://doi.org/10.1016/j.envpol.2015.08.009, 2015.

Sugita, S.: Pollen representation of vegetation in Quaternary sediments: Theory and method in patchy vegetation, J. Ecol., 82, 881–897, DOI: https://doi.org/10.2307/2261452, 1994.

van der Werf, G. R., Randerson, J. T., Giglio, L., Collatz, G. J., Mu, M., Kasibhatla, P. S., Morton, D. C., DeFries, R. S., Jin, Y., and van Leeuwen, T. T.: Global fire emissions and the contribution of deforestation, savanna, forest, agricultural, and peat fires (1997–2009), Atmos. Chem. Phys., 10, 11707-11735, DOI:10.5194/acp-10-11707-2010, 2010.

van der Werf, G. R., Peters, W., van Leeuwen, T. T., and Giglio, L.: What could have caused pre-industrial biomass burning emissions to exceed current rates? Clim. Past, 9, 289–306, DOI:10.5194/cp-9-289-2013, 2013.

Wang, Z., Chappellaz, J., Park, K., and Mak, J.E.: Large variations in southern hemisphere biomass burning during the last 650 years, Science 330, 1663-1666, DOI: 10.1126/science.1197257, 2010.

Ward, D. S., Kloster, S., Mahowald, N. M., Rogers, B. M., Randerson, J. T., and Hess, P. G.: The changing radiative forcing of fires: global model estimates for past, present and future, Atmos. Chem. Phys., 12, 10857–10886, DOI:10.5194/acp-12-10857-2012, 2012.

Wenzel, S., Cox, P. M., Eyring, V. ,and Friedlingstein, P.: Emergent constraints on climate-carbon cycle feedbacks in the CMIP5 Earth system models, J. Geophys. Res. – Biogeosci., 119, 794–807, DOI:10.1002/2013JG002591, 2014.

Earth Syst. Dynam. Discuss., https://doi.org/10.5194/esd-2018-11
Manuscript under review for journal Earth Syst. Dynam.
Discussion started: 26 February 2018

Earth System Dynamics
Discussions
Open Access

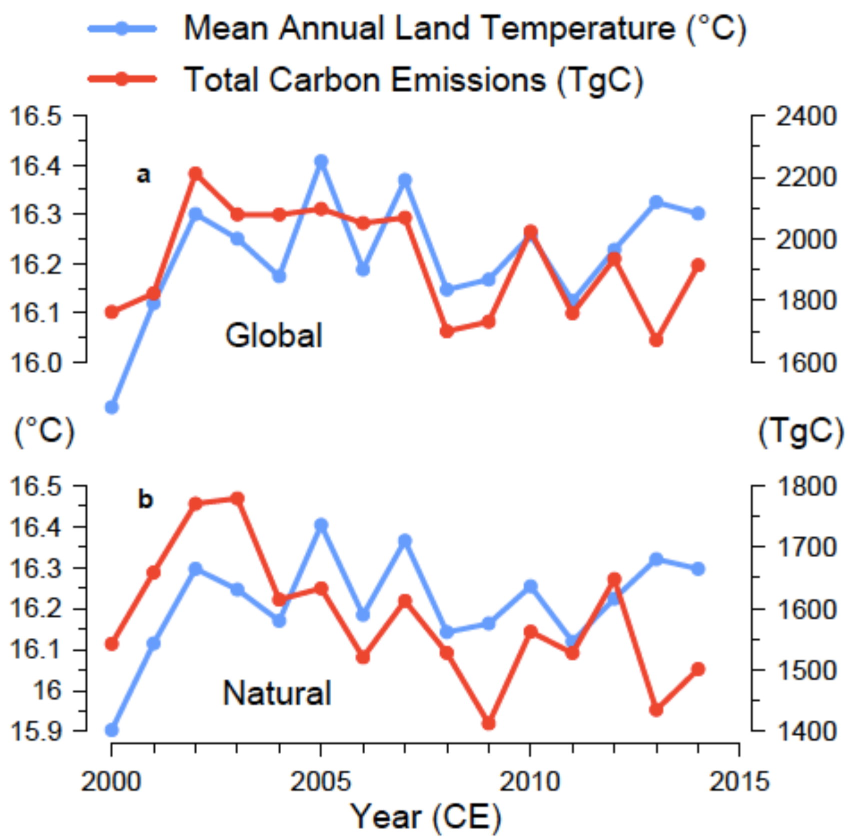

Figure 1: Co-evolution of temperature and fire-related emissions over the period between 2000 and 2014. The temperature data are from the NOAA data set (ftp://ftp.ncdc.noaa.gov/pub/data/anomalies/anomalies/usingGHCNMv2/annual.land_ocean.90S.90N.df_1901-2000mean.dat) and the emissions data are from GFED4 (Randerson et al., 2015, www.globalfiredata.org). The top panels show global (a) temperature and (b) emissions after excluding agricultural areas; the bottom panels show (c) temperature and (d) emissions from areas of natural vegetation only, excluding both deforestation fires and peatland fires.

Earth Syst. Dynam. Discuss., https://doi.org/10.5194/esd-2018-11
Manuscript under review for journal Earth Syst. Dynam.
Discussion started: 26 February 2018

Earth System Dynamics
Discussions
Open Access

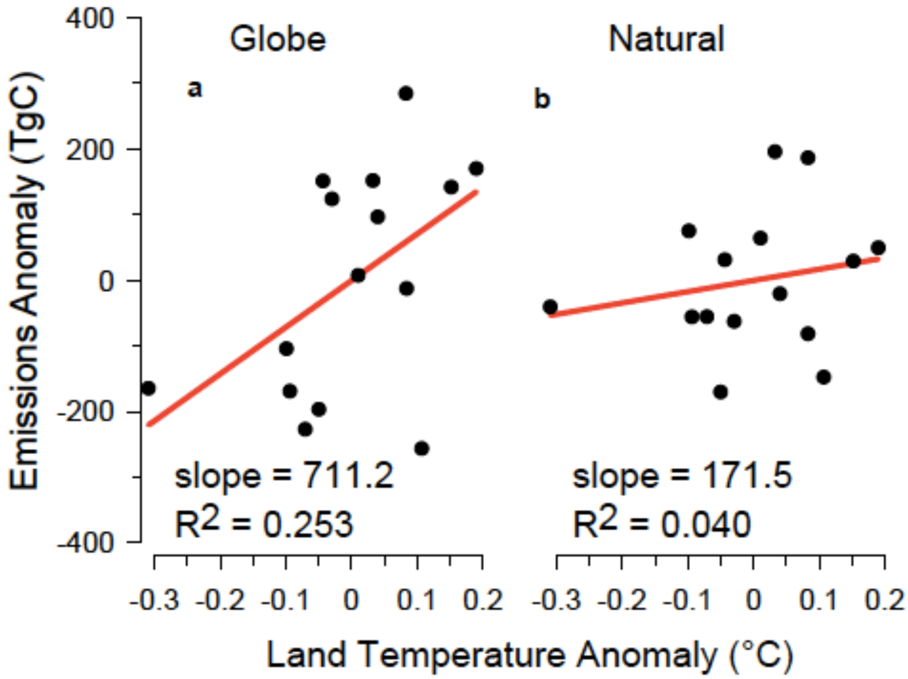

Figure 2: Relationship between global fire-related emissions and temperature over the period between 2000 and 2014. The left-hand panel shows the relationship between global temperature and emissions after excluding agricultural areas; the right-hand panel shows the relationship between temperature and emissions from areas of natural vegetation only, excluding both deforestation fires and peatland fires.

Earth Syst. Dynam. Discuss., https://doi.org/10.5194/esd-2018-11
Manuscript under review for journal Earth Syst. Dynam.
Discussion started: 26 February 2018

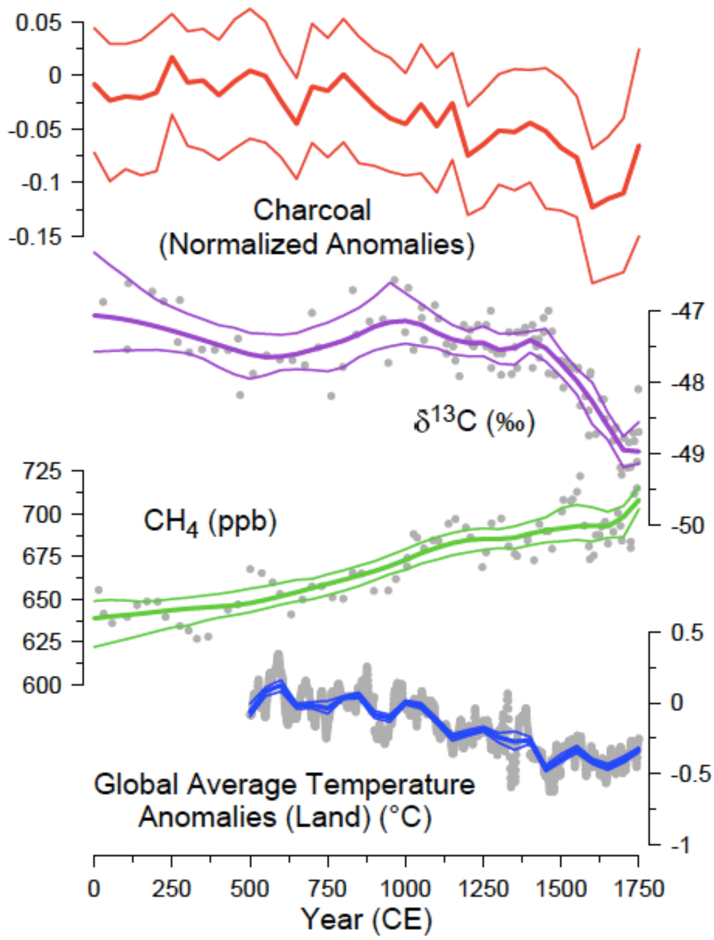

Figure 3: Indices of pre-industrial global biomass burning trends, 0–1750 CE: (a) normalised charcoal anomalies, (b) $\delta^{13}C$ of CH_4 (‰) based on a composite of the data from Ferretti et al (2005), Mischler et al. (2009) and Sapart et al. (2012), and (c) CH_4 concentration (ppb) from Etheridge et al. (2010). The bottom plot shows global average temperature anomalies over land (°C) from Mann et al. (2009). The plots show the 50-year smoothed record for each indicator, with 95% bootstrap confidence intervals; the individual data points for $\delta^{13}C$, CH_4 and land temperature are shown by grey points. There are too many individual charcoal points to be shown.

Earth Syst. Dynam. Discuss., https://doi.org/10.5194/esd-2018-11
Manuscript under review for journal Earth Syst. Dynam.
Discussion started: 26 February 2018

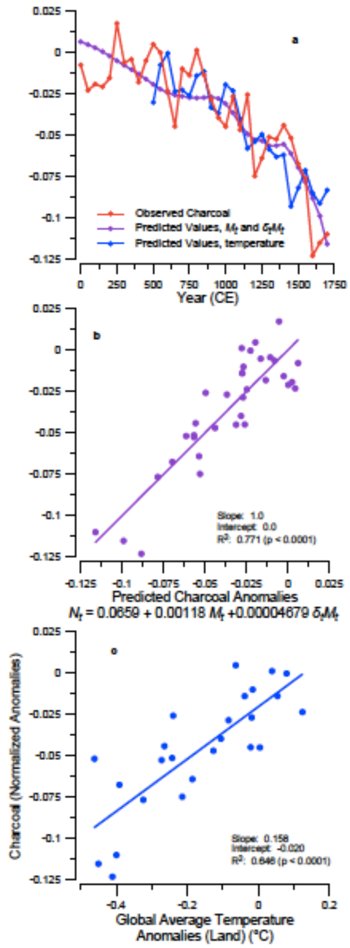

Figure 4: Relationship between normalized charcoal anomalies and global land temperature. The data points refer to 50-year binned data. The top panel (a) shows observed charcoal normans; estimated values based on the linear regression of charcoal normans against the $\delta^{13}C$ of CH_4 and the product of this $\delta^{13}C$ value with the concentration of CH_4, as plotted in (b); and estimated values based on the linear regression of charcoal normans against temperature, as plotted in (c). Note that the slope and intercept of the relationship shown in panel (b) are necessarily 1.0 and 0.0, respectively – the key point is the goodness of fit shown between the two data sources after the charcoal data have been calibrated against the CH_4 and CH_4 isotopic records.